Applied Physics Letters

Statistics of electrical breakdown field in HfO_2 and SiO_2 films from millimeter to nanometer length scales

Cite as: Appl. Phys. Lett. **91**, 242905 (2007); https://doi.org/10.1063/1.2822420
Submitted: 12 September 2007 • Accepted: 15 November 2007 • Published Online: 14 December 2007

Cédric Sire, Serge Blonkowski, Michael J. Gordon, et al.

AIP Publishing

Statistics of electrical breakdown field in HfO_2 and SiO_2 films from millimeter to nanometer length scales

Cédric Sire[a] and Serge Blonkowski
ST Microelectronics, 850 rue Jean Monnet, 38926 Crolles Cedex, France

Michael J. Gordon[b] and Thierry Baron
Laboratoire des Technologies de la Microélectronique (CNRS-LTM), 17 Avenue des Martyrs, 38054 Grenoble, France

(Received 12 September 2007; accepted 15 November 2007; published online 14 December 2007)

The statistics of electrical breakdown field (E_{bd}) of HfO_2 and SiO_2 thin films has been evaluated over multiple length scales using macroscopic testing of standardized metal-oxide-semiconductor ($TiN/SiO_2/Si$) and metal-insulator-metal ($TiN/HfO_2/TiN$) capacitors (10^{-2} mm^2–10 μm^2 area) on a full 200 mm wafer along with conductive-atomic-force microscopy. It is shown that E_{bd} follows the same Weibull distribution when the data are scaled using the testing area. This overall scaling suggests that the defect density is $\sim 10^{15}$ cm^{-2} and E_{bd} is $\sim$40 MV/cm for nanometer-length scales; as such, breakdown in these materials is most likely initiated by bond breaking rather than punctual defects. © *2007 American Institute of Physics*. [DOI: 10.1063/1.2822420]

Dielectric materials with higher permittivity than SiO_2 are being investigated as gate insulators in metal-oxide-semiconductor (MOS) devices[1] and for metal-insulator-metal (MIM) capacitors used in dynamic random access memory[2] and rf applications.[3] In the case of MOS devices, a thicker dielectric layer (2–3 nm) can be used to prevent electron tunneling, but the overall capacitance must be kept the same as 1–1.5 nm thick SiO_2. Due to these demanding requirements, new high-K oxide materials such as HfO_2, ZrO_2, and HfSiO are being explored as alternatives.[4] Decreasing device dimensions also require more detailed understanding of electrical breakdown at the nanoscale. Unfortunately, breakdown fields in high-K materials have generally been shown to be lower than in SiO_2.[5] In this letter, we compare the statistical distributions of breakdown electric field (E_{bd}) for different dielectrics (SiO_2 and HfO_2) using macroscopic *IV* (current versus voltage) tests on standardized capacitors ($\geqslant$100 μm^2) with nanoscale measurements using conductive-atomic-force microscopy (C-AFM) under UHV. *IV* curves and E_{bd} were measured with both methods for different oxide thicknesses (1.2–6 nm) on p- and n-type Si (MOS structures) as well as TiN/oxide/TiN stacks (MIM capacitors). High defect densities (10^{15} cm^{-2}) and large fields (40 MV/cm) suggest that breakdown in high-K materials at the nanoscale occurs via bond breaking rather than punctual defects such as vacancies and interstitials.

Electrical breakdown measurements on high-K materials typically show much lower fields (E_{bd}) than for SiO_2 of comparable thickness.[5] This observation is usually explained by the presence of a larger local electric field on chemical bonds when the dielectric constant is high. However, the statistical mean value of E_{bd} is seen to increase substantially when the surface area for testing decreases. This latter effect can be explained by the probability of finding a defect which leads to breakdown: larger surface area mean higher overall probability. In order to investigate the inherent density and role of defects, it is common to measure the statistical distribution of E_{bd} for very small (nanoscale) surface areas. For this, conductive-atomic-force microscopy (C-AFM) electrical measurements have been successfully used as a local electrical probe for thin SiO_2.[6–8] In particular, the local breakdown properties of Si/SiO_2 at nanometer scales have been the subject of several extensive studies.[9–12] Recently, time-dependent dielectric breakdown (TDDB) measurements on $SiO_2/4H$-SiC with C-AFM showed good agreement with measurements performed on "standardized" SiO_2/Si capacitors.[13] Comparable agreements of the dielectric breakdown kinetics have been observed with Pr_2O_3 on Si, and it was demonstrated that C-AFM was a reliable approach for characterizing TDDB events.[14]

In the present study, macroscopic breakdown tests were carried out on two dielectric films: 3 nm SiO_2 (thermally grown) on Si (2×10^{19}, n type) and 4 nm HfO_2 (atomic layer deposition) on TiN using $TiN/SiO_2/Si$ and $TiN/HfO_2/TiN$ standardized capacitors, respectively.[15] Electrical measurements were made with a four-point probe station and Hewlett-Packard 4192 picoampere meter on 68 different capacitors (areas from 100 to 80 000 μm^2), distributed randomly over a full 200 mm Si wafer.

C-AFM electrical measurements were performed with an Omicron AFM/scanning tunneling microscopy system under UHV conditions ($<10^{-9}$ torr) with conductive diamond tips (B doped).[16] The AFM tip served as the top electrode for the "test" capacitor and voltage was applied to the substrate with the tip at virtual ground (i.e., the tip was connected to an in-vacuum current preamplifier referenced to ground). Electrical contact between sample and stage was assured with indium solder, and all samples were outgassed at 250 °C for 3 h at $<10^{-8}$ torr. *IV* measurements were carried out on a 9×9 grid in contact mode (normal force=20 nN) with the *XY* scanning of the AFM tip stopped. Reproducibility of the tip-surface electrical contact was investigated with respect to contact force; above a particular threshold (20 nN), *IV* traces and E_{bd} were seen to be contact-force invariant.

Figure 1 shows a topographic image (1.5×1.5 μm^2) of a 2 nm thick SiO_2 layer after a 9×9 grid of breakdown test

[a]Electronic mail: cedric.sire@cea.fr
[b]Present address: Deptartment of Chemical Engineering, University of California-Santa Barbara, Santa Barbara, CA 93106-5080.

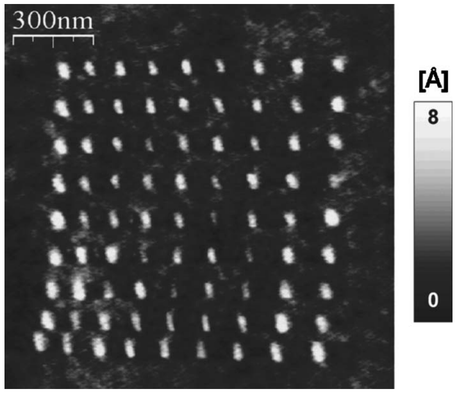

FIG. 1. AFM topography image taken after a 9×9 *IV* grid on a 2 nm thick SiO_2 film thermally grown on a Si substrate.

points was measured. Bright spots in the image correspond to the location of the *IV* test; the topographic "bump" ($\sim$8 Å) is due to trapped negative charges that give rise to an additional electrostatic force on the AFM tip causing the tip to pull away slightly to maintain constant force feedback.[17–19] Typical *IV* traces for the grid experiment are shown in Fig. 2 for 4 nm HfO_2 on TiN, where positive bias represents electron injection from the AFM tip (i.e., the "gate" electrode). Five *IV* traces are superposed to represent measurement dispersion. In these evaluations, breakdown voltage was defined as the point when the *IV* slope became infinite (arrow on Fig. 2). Similar macroscopic *IV* tests (not show) were conducted on the same films using standardized capacitors in the MOS or MIM configurations discussed earlier.

Figure 3 shows a comparison of the cumulative breakdown probability versus voltage for the macro- and AFM-based measurements of 4 nm HfO_2 on TiN. Capacitor areas for macrotesting ranged from 100 to 10^4 μm^2. As expected, the mean breakdown voltage is much larger ($\sim$5 times) for the AFM test compared to the 10^4 μm^2 capacitor. The cumulative probability (P which represent the likelihood that huge currents will flow at a particular applied voltage) variation with breakdown voltage (V_{bd}) or field (E_{bd}) can be fit with a Weibull distribution,

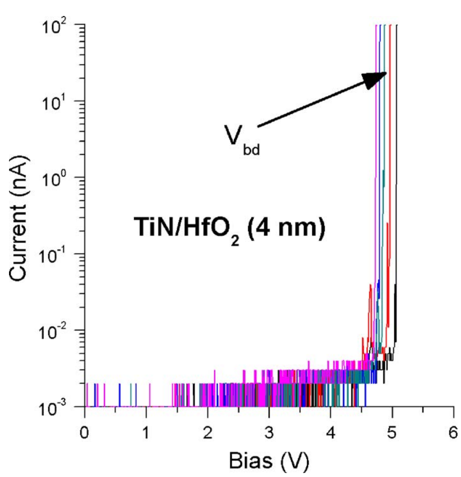

FIG. 2. (Color online) Five superposed nanometric *IV* characteristics measured by C-AFM on a 4 nm HfO_2/TiN MIM structure.

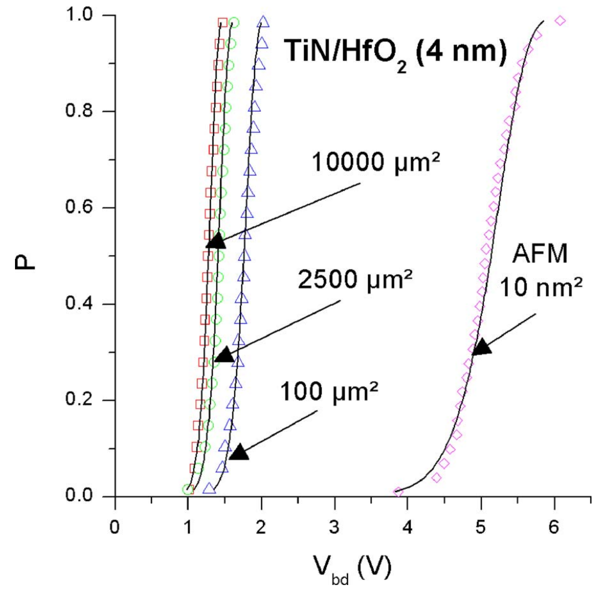

FIG. 3. (Color online) Cumulative probability of breakdown for 4 nm thick HfO_2 on TiN, comparing macro—(standard capacitors) and nanotesting (C-AFM). Lines are fits to a Weibull distribution [Eq. (1)].

$$P = 1 - \exp\left[-\left(\frac{E_{bd}}{E_0}\right)^{\beta}\frac{S}{S_0}\right] = 1 - \exp\left[-\left(\frac{V_{bd}}{V_0}\right)^{\beta}\frac{S}{S_0}\right]. \quad (1)$$

Here, S is the capacitor surface area, S_0 is a reference surface area, and β and E_0 (or V_0) are the Weibull parameters. Taking the reference surface $S_0=10^4$ μm^2, one can determine V_0 and β using other surface areas (100 and 2500 μm^2, respectively). Once the Weibull parameters are known from macroscopic testing, the corresponding tip-surface contact area for the C-AFM measurement can be determined (10 ± 5 nm^2). This value is quite reasonable, as estimated from scanning electron microscopy (SEM) images of the tip end and AFM topographic images of Si nanocrystals. In the latter case, 10 nm structures with spacings of 20–100 nm could easily be resolved with the diamond-coated tip used for *IV* testing. In addition, Olbrich *et al.* measured tip radii on the order of 10–20 nm at the apex by SEM.[16]

The aforementioned analysis was applied to different dielectrics (SiO_2 and HfO_2) to evaluate whether a single Weibull scaling law can explain breakdown results from the macro- to nanoscales. Figure 4 shows another Weibull plot for SiO_2 and HfO_2 where the data for all surface areas are compared. In this case, individual Weibull plots (i.e., Fig. 3) are condensed to a "cumulative" probability of breakdown for each film by linearizing Eq. (1) and taking probability ratios (P_1 and P_2) for different surface areas (S_1 and S_2),

$$\ln[-\ln(1-P_1)] - \ln[-\ln(1-P_2)] = \ln\left(\frac{S_1}{S_2}\right). \quad (2)$$

When this relation is applied to all the data for a particular film, a straight line is seen (Fig. 4). The fitted surface area for SiO_2/Si is seen to be $\sim$10 times lower than that for HfO_2/TiN. This difference is likely due to surface roughness of the substrate being transferred to the dielectric film during growth. HfO_2 surfaces had a rms roughness of $\sim$1 nm, while the SiO_2 was exceptionally smooth (rms roughness $<$0.1 nm). Since the tip apex could penetrate into larger "valleys" on the HfO_2 surface (i.e., the lateral wavelength of

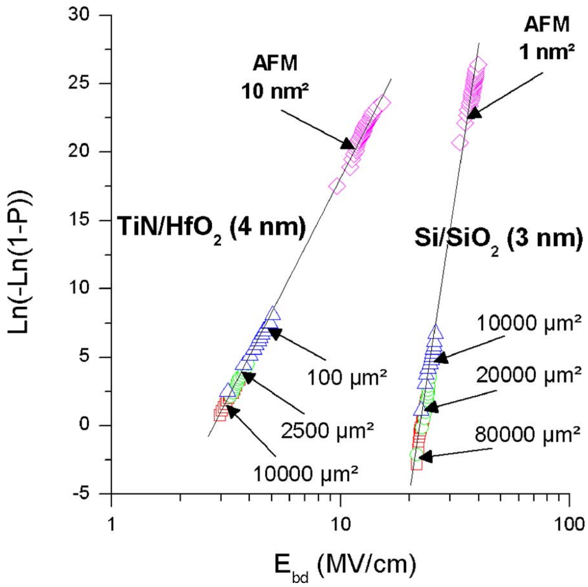

FIG. 4. (Color online) Weibull plot of the breakdown electric field distribution for 3 nm SiO_2/Si and 4 nm HfO_2/TiN for different surface areas of testing, normalized to the largest area (800 00 μm^2).

surface roughness was $\sim$25 nm for HfO_2, close to the tip diameter), the contact surface would be larger for HfO_2 compared to the smoother SiO_2 surface.

The linear nature of the Weibull plots in Fig. 4 for both materials strongly suggests that breakdown occurs via the same mechanism for testing areas of 10 nm^2 all the way up to 0.01 mm^2 with the Weibull slope $\beta=44$ for Si/SiO_2 and $\beta=14.4$ for TiN/HfO_2. Higher β indicates a lower dispersion of E_{bd} for SiO_2. The lower β value for HfO_2 may also be explained by the roughness effect. Weibull statistics arise from the assumption that the density of defects (which generate breakdown) is identical for all surface areas tested. With respect to the C-AFM breakdown measurements, surfaces in the 1–10 nm^2 range were seen to follow the same Weibull trend. As such, it would be safe to assume that the density of defects must be at least an order of magnitude greater than the tip-surface area during the test. This being said, 10–100 defects in a surface area of 1–10 nm^2 leads to $\sim 10^{15}$ defects/cm^2—on the same order as the surface atomic density. We can likewise estimate the volume density of defects using the tip-surface contact area and film thickness. For this case, 100 defects in a volume of 3 nm^3 correspond to 5×10^{22} defects cm^{-3}, which is nearly equivalent to the atomic density. The mean E_{bd} measured via C-AFM should not be far from the "intrinsic" value. For HfO_2 (SiO_2), E_{bd} approaches 13 MV/cm (40 MV/cm) at the nanometer scale, whereas standard device measurements typically show $\sim$4 MV/cm (23 MV/cm). E_{bd} is largest for the smallest surface, with breakdown in HfO_2 at significantly lower fields than SiO_2; the latter is in agreement with the value given by McPherson ($\sim$30 MV/cm is needed to break bonds in SiO_2).[20] A plot similar to that of Fig. 4 can be drawn by replacing E_{bd} with an equivalent oxide breakdown field using $E_{bd\text{-}EOT}$ (defined as V_{bd}/EOT), where EOT the effective oxide thickness is $3.9/K$ times the physical film thickness, K being the dielectric constant. In this case, β and the local contacting surface area remain unchanged, but $E_{bd\text{-}EOT}=E_{bd}\times(K/3.9)$, with $K=17$ for HfO_2. In this case, the equivalent oxide breakdown fields are $E_{bd\text{-}EOT}\sim 15$ MV/cm at the macroscopic scale and $E_{bd\text{-}EOT}\sim 60$ MV/cm at the nanometer scale.

In terms of a charge percolation model,[21] our results indicate that nearly any atomic bond is a potential breakdown path. With such a hypothesis, electrical breakdown in these films would be initiated by bond breaking rather than by extrinsic defects such as vacancies or interstitials. Another recent study[5] on SiO_2 has shown breakdown fields of $\sim$30 MV/cm which is very near the bond-breaking limit for Si–O.[20] Additionally, the present work demonstrates that AFM-based statistical testing is a viable, informative, and potentially easier alternative to macroscopic electrical testing which may require more processing steps (such as lithography, etching, electrode deposition, etc.).

The authors would like to especially acknowledge J. F. Damlencourt and Y. Campidelli for deposition as well as Y. Morand and S. Descombes for sample integration.

[1] G. D. Wilk, R. M. Wallace, and J. M. Anthony, J. Appl. Phys. **89**, 5243 (2001).
[2] Y. Aoki, T. Ueda, H. Shirai, T. Sakoh, T. Kitamura, and S. Arai, Tech. Dig. - Int. Electron Devices Meet. **2002**, 831.
[3] H. Hu, C. Zhu, Y. F. Lu, B. J. Cho, and W. K. Choi, IEEE Electron Device Lett. **23**, 514 (2002).
[4] G. Ribes, J. Mitard, M. Denais, S. Bruyere, F. Monsieur, C. Parthasarathy, E. Vincent, and G. Ghibaudo, IEEE Trans. Device Mater. Reliab. **5**, 5 (2005).
[5] J. W. McPherson, J. Kim, A. Shanware, H. Mogul, and J. Rodriguez, IEEE Trans. Electron Devices **50**, 1771 (2003).
[6] A. Olbrich, B. Ebersberger, and C. Boit, Proceedings of the 36th IEEE Annual International Reliability Physics Reno, 1998 (unpublilshed), p. 163.
[7] A. Olbrich, B. Ebersberger, and C. Boit, Appl. Phys. Lett. **73**, 3114 (1998).
[8] M. Porti, M. Nafria, X. Aymerich, A. Olbrich, and B. Ebersberger, Appl. Phys. Lett. **78**, 4181 (2001).
[9] M. Porti, M. Nafría, X. Aymerich, A. Olbrich, and B. Ebersberger, J. Appl. Phys. **91**, 2071 (2002).
[10] M. Porti, R. Rodrigez, M. Nafria, X. Aymerich, A. Olbrich, and B. Ebersberger, J. Non-Cryst. Solids **280**, 138 (2001).
[11] M. Porti, R. Rodrigez, M. Nafria, X. Aymerich, A. Olbrich, and B. Ebersberger, Microelectron. Eng. **59**, 265 (2001).
[12] A. Ando, K. Miki, and K. Sakamoto, Proceedings of the IWGI Tokyo, 2001 (unpublished), p. 124.
[13] P. Fiorenza and V. Raineri, Appl. Phys. Lett. **88**, 212112 (2006).
[14] P. Fiorenza, R. Lo Nigro, V. Raineri, and S. Salvatore Lombardo, Appl. Phys. Lett. **87**, 231913 (2005).
[15] F. Mondon and S. Blonkowski, Microelectron. Reliab. **43**, 1259 (2003).
[16] A. Olbrich, B. Ebersberger, and C. Boit, J. Vac. Sci. Technol. B **17**, 1570 (1999).
[17] M. Porti, M. Nafria, M. C. Blum, and X. Aymerich, Appl. Phys. Lett. **81**, 3615 (2002).
[18] A. Neugroschel, L. Wang, and G. Bersuker, J. Appl. Phys. **96**, 3388 (2004).
[19] M. J. Gordon and T. Baron, Phys. Rev. B **72**, 165420 (2005).
[20] J. W. McPherson, J. Appl. Phys. **95**, 8101 (2004).
[21] J. H. Stathis, J. Appl. Phys. **86**, 5757 (1999).